Fermi National Accelerator Laboratory

FERMILAB-Pub-93/184-E
E687

A Measurement of $\Gamma(\mathbf{D}_s^+ \to \phi\mu^+\upsilon)/\Gamma(\mathbf{D}_s^+ \to \phi\pi^+)$

P.L. Frabetti et al
The E687 Collaboration

Fermi National Accelerator Laboratory
P.O. Box 500, Batavia, Illinois 60510

July 1993

Submitted to *Physics Letters B*

Operated by Universities Research Association Inc. under Contract No. DE-AC02-76CHO3000 with the United States Department of Energy

Disclaimer

A Measurement of $\Gamma(D_s^+ \to \phi\mu^+\nu)/\Gamma(D_s^+ \to \phi\pi^+)$

P. L. Frabetti

Dip. di Fisica dell'Università and INFN - Bologna, I-40126 Bologna, Italy

H. W. K. Cheung, J. P. Cumalat, C. Dallapiccola [a], J. F. Ginkel, S. V. Greene,

W. E. Johns, M. S. Nehring

University of Colorado, Boulder, CO 80309, USA

J. N. Butler, S. Cihangir, I. Gaines, P. H. Garbincius, L. Garren, S. A. Gourlay,

D. J. Harding, P. Kasper, A. Kreymer, P. Lebrun, S. Shukla, M. Vittone

Fermilab, Batavia, IL 60510, USA

S. Bianco, F. L. Fabbri, S. Sarwar, A. Zallo

Laboratori Nazionali di Frascati dell'INFN, I-00044 Frascati, Italy

R. Culbertson, R. W. Gardner, R. Greene, J. Wiss

University of Illinois at Urbana-Champaign, Urbana,IL 61801

G. Alimonti, G. Bellini, B. Caccianiga, L. Cinquini [b], M. Di Corato, M. Giammarchi,

P. Inzani, F. Leveraro, S. Malvezzi [c], D. Menasce, E. Meroni, L. Moroni, D. Pedrini,

L. Perasso, A. Sala, S. Sala, D. Torretta [d]

Dip. di Fisica dell'Università and INFN - Milano, I-20133 Milan, Italy

D. Buchholz, D. Claes [e], B. Gobbi, B. O'Reilly,

Northwestern University, Evanston, IL 60208, USA

J. M. Bishop, N. M. Cason, C. J. Kennedy [f], G. N. Kim, T. F. Lin, D. L. Puseljic,

R. C. Ruchti, W. D. Shephard, J. A. Swiatek, Z. Y. Wu

University of Notre Dame, Notre Dame, IN 46556, USA

V. Arena, G. Boca, C. Castoldi, G. Gianini, S. P. Ratti, C. Riccardi, P. Vitulo

Dip. di Fisica Nucleare e Teorica and INFN - Pavia, I-27100 Pavia, Italy

A. Lopez, University of Puerto Rico at Mayaguez, Puerto Rico

G. P. Grim, V. S. Paolone, P. M. Yager, University of California-Davis, Davis, CA 95616

J. R. Wilson, University of South Carolina, Columbia, SC 29208

P. D. Sheldon, Vanderbilt Univeristy, Nashville, Tenn.,TN 37235 USA

F. Davenport, University of North Carolina-Asheville, Asheville, NC 28804

J. F. Filaseta, Northern Kentucky University, Highland Heights, KY 41076

G.R. Blackett, M. Pisharody, T. Handler

University of Tennessee, Knoxville, TN 37996 USA

B. G. Cheon, J. S. Kang, K. Y. Kim

Korea University, Seoul 136-701, Korea

Abstract

Fermilab high-energy photoproduction experiment E687 measures a branching ratio of $\Gamma(D_s^+ \to \phi\mu^+\nu)/\Gamma(D_s^+ \to \phi\pi^+) = 0.58 \pm 0.17$ (stat) $\pm$ 0.07 (sys). This branching ratio is combined with theoretical inputs to obtain a new measurement of the D_s^+ absolute branching ratio of $\Gamma(D_s^+ \to \phi\pi^+)/\Gamma(D_s^+ \to$ all $) = 0.031 \pm 0.009$(stat) $\pm$ 0.005 (sys) $\pm$ 0.004 (theoretical).

We report on a new measurement of the branching ratio $\Gamma(D_s^+ \to \phi\mu^+\nu)$ / $\Gamma(D_s^+ \to \phi\pi^+)$ using data collected in the photoproduction experiment E687, conducted in the Fermilab Wideband Photon beam during the 1990-1991 fixed-target run. This branching ratio is of particular interest since it provides information on the absolute branching ratio for $D_s^+ \to \phi\pi^+$ when combined with information on the D_s^+ lifetime, the well measured $\Gamma(D^+ \to \overline{K}^{*0}\mu\nu)$ partial width, and the theoretical expectations [1] [2] that $\Gamma(D_s^+ \to \phi\mu^+\nu) \approx \Gamma(D^+ \to \overline{K}^{*0}\mu^+\nu)$.

This analysis is based on a sample of approximately 100 $D_s^+ \to \phi\mu^+\nu$ candidates (charge conjugates are implied). Because of the missing neutrino, the final state is only partially reconstructed and this sample includes backgrounds from charm final states which include a ϕ and either a muon or a misidentified muon along with additional undetected particles. We show later how these backgrounds can be estimated from measured branching ratios and limits, theoretical expectations, and a fit to the decay kinematic variables.

The E687 detector [3] measures high-energy photon-Beryllium interactions using a multiparticle magnetic spectrometer with excellent vertex measurement, particle identification, and calorimetric capabilities. The average triggered photon energy is approximately 220 GeV. Charged particles emerging from the experimental target are tracked through a silicon microstrip vertex detector, an analysis magnet, three stations of multiwire proportional chambers, a second analysis magnet, and two more multiwire proportional chambers. The vertex detector measures decay proper times with 0.048 ps resolution for charm particles which decay with all daughters detected in the microstrips. Three Čerenkov counters with different thresholds allow kaons to be separated from pions over a momentum range from 4.5 to 61 GeV/c. Particle tracks are projected through the inner electromagnetic calorimeter, hadron calorimeter, and additional shielding and are matched to hits in the inner muon detector consisting of three planes of scintillators and four planes of 5.08 cm diameter proportional tubes, covering approximately $\pm$ 40 mrad.

Many of the techniques and analysis cuts used here are similar to those employed for our analysis [4] of the decay $D^+ \to \overline{K}^{*0}\mu^+\nu$. The data were reconstructed and selected by

requiring evidence of detached vertices in the event. Specifically, all high-quality two-track vertices were formed and the event was accepted for final processing if any two vertices were separated by more than 4.5σ. All tracks found in both the MWPC and microstrip system are searched for the correct sign, mass, lepton and Čerenkov identification combinations to form $K^+K^-\mu^+$ candidates.

The muon is identified in the inner muon detector where it must leave hits in at least three of the seven planes if the momentum is less than 30 GeV/c, and at least five of the seven planes if the momentum is greater than 30 GeV/c. The kaons must be identified by the Čerenkov system as kaon definite or kaon-proton ambiguous. To avoid possible contamination from diffractively photoproduced ϕ's , we require that the value of $p_\perp^2$ for the ϕ with respect to the incident photon direction exceeds $0.05\mathrm{GeV}^2/\mathrm{c}^2$. Finally to eliminate backgrounds from $D_s^+ \to \phi\pi^+$ decay we require that the $\phi\mu$ invariant mass be less than 1.9 $\mathrm{GeV}/\mathrm{c}^2$.

We require that the $K^+K^-\mu^+$ combination originates from a common point by requiring a good confidence level for the three-track secondary vertex. The main technique for eliminating non-charm backgrounds is to require a statistically significant detachment of the secondary vertex from the production vertex. We find the production vertex by searching for the most upstream high-quality vertex in the target region containing two or more tracks that can be made from the tracks which remain after the $K^+K^-\mu^+$ combination is removed. Defining the distance between the production and secondary vertices by ℓ and its measurement error by σ, we require detachment by cutting on the normalized separation between the primary and secondary vertices, ℓ/σ. Finally, we require that the $K^+K^-\mu^+$ vertex be isolated from other tracks in the event (not including tracks in the primary vertex) by requiring that the maximum confidence level for another track to form a vertex with the candidate be less than 10%.

Figure 1 shows the K^+K^- invariant mass distribution for $K^+K^-\mu^+$ candidates with a secondary vertex confidence level exceeding 20% for several ℓ/σ cuts. The peak due to $\phi(1020) \to K^+K^-$ is clearly visible. The displayed curve is the result of a fit to the K^+K^-

mass spectrum to a resolution-broadened P-wave Breit-Wigner ϕ peak over a polynomial background. Figure 2a shows that the yield of $\phi\mu$ events as a function of the ℓ/σ cut follows the predictions of a $D_s^+ \to \phi\mu^+\nu$ Monte Carlo simulation generated with the present measured [1] lifetime of the D_s^+. Figure 2b compares the fitted ϕ yield for events satisfying the detachment cut $\ell/\sigma > 3$ as a function of the minimum confidence level requirement on the secondary vertex to the predictions of our $D_s^+ \to \phi\mu^+\nu$ Monte Carlo simulation. The accumulation of events at low secondary vertex confidence levels suggests substantial contamination from events where the ϕ and muon did not originate from the same decay vertex. This accumulation observed in the data is partially reproduced by a general photoproduction Monte Carlo where all charm species and known decay modes are simulated for both the charm and anticharm particle (dashed curve). This suggests that some of the low confidence level accumulation is due to charm backgrounds where a muon from one charm decay is combined with a ϕ from the other charm decay. A strong contamination from low quality $\phi\mu$ vertices was also observed by the E691 collaboration [5]. To significantly reduce this contamination, we require that the secondary vertex confidence level exceeds 20%.

We investigated possible contaminations from D^+ and D_s^+ decays which include a ϕ along with either a real muon or a track which is misidentified as a muon*. Three of these backgrounds, $D_s^+ \to \phi\pi^+\pi^0$, $D^+ \to \phi\pi^+\pi^0$, $D_s^+ \to \phi\pi^+\pi^-\pi^+$ can be estimated from their known [1] branching ratios and our measurements of the probability that a pion is misidentified as a muon ($1.0 \pm 0.1\%$), and our estimates† of the relative production rates of the D^o , D^+ , and D_s^+. These three backgrounds are expected to contribute relative to

---

*Less than two events are expected to come from the combined dominant D^o background sources of $\phi\pi^+\pi^-$ and $\phi\pi^+\pi^-\pi^o$.

†We estimate a D_s^+/D^+ production ratio of 0.6 ± 0.2 by comparing the observed yields of D_s^+ and $D^+ \to K^+K^-\pi^+$ and correcting for acceptance and the known [1] branching ratios. We estimate a D_s^+/D^o production ratio of 0.17 ± 0.05 where we used the $K^-\pi^+$ decay mode for the D^o.

the $D_s^+ \to \phi\mu^+\nu$ with ratios of 0.06 $\pm$ 0.04, 0.05 $\pm$ 0.03, and 0.004 $\pm$ 0.002 respectively. This leaves three potential background sources with no measured branching ratios: $D_s^+ \to \phi\pi^0\mu^+\nu$, $D^+ \to \phi\mu^+\nu$, and $D^+ \to \phi\overline{K}^0\mu^+\nu$. The first two of these are expected [6] to be negligible because they are OZI suppressed. There exists an experimental upper limit [1] on the branching ratio for $D^+ \to \phi\mu^+\nu$ decay. However, there are no existing experimental constraints on possible contamination from the decays $D_s^+ \to \phi\pi^0\mu^+\nu$ or $D^+ \to \phi\overline{K}^0\mu^+\nu$.

To estimate the true level of the $D_s^+ \to \phi\mu^+\nu$ signal, we fit the distributions of four kinematic variables measured for the $\phi\mu^+\nu$ candidates to a linear combination of the distributions predicted for the signal and the six non-negligible background sources. A binned likelihood fit was performed to the kinematic variable distributions where the six fit parameters were the fraction of $\phi\mu^+\nu$ candidates due to each background source.[‡] Information for each background with an estimated yield was included in this fit with an additional Gaussian factor.

The four kinematic variables were chosen to differentiate the $D_s^+ \to \phi\mu^+\nu$ signal from various background contributions. We use the $\phi\mu$ invariant mass, $M(\phi\mu)$, to differentiate the signal from charm decays with additional, unobserved particles at the $\phi\mu$ vertex which will tend to have a softer distribution than the signal. In order to provide discrimination against D^+ decays, we use the reconstructed proper time[§] as the second kinematic variable. Finally we have attempted to exploit the expectation [7] that $D_s^+ \to \phi\mu^+\nu$ decays should be governed

---

[‡]In the fit we allowed for non-ϕ backgrounds by adding to the prediction the joint distribution from two symmetrically placed, 6 MeV/c^2 wide sidebands about the ϕ peak.

[§]Because of the missing neutrino, the momentum of the D_s^+ candidate is reconstructed by requiring that it lies along the line defined by the primary and secondary vertices. This leaves a two-fold ambiguity which is resolved by using the solution which gives the lower D_s momentum as was done in our analysis [4] of the $D^+ \to \overline{K}^{*0}\mu^+\nu$ final state.

by form factor ratios which are nearly identical to those measured [4] for $D^+ \to \overline{K}^{*0}\mu^+\nu$. ** We include two angular variables which are $\cos\theta_v$, the angle between the K^+ and the D_s direction in the ϕ rest frame, and $\cos\theta_\mu$, the angle between the ν and the D_s direction in the $\mu\nu$ rest frame. The fit is to the joint distribution of $M(\phi\pi)$, $\cos\theta_v$, and $\cos\theta_\mu$ and the projection of the proper time since we expect the proper time to be uncorrelated with the other variables. The $D^+ \to \phi\mu^+\nu$ decay is simulated using the same intensity expression as the $D_s^+ \to \phi\mu^+\nu$ signal††. The five remaining background contributions were simulated with a phase space decay intensity.

As a way of illustrating the discrimination power of the three kinematic variables, we compare Monte Carlo predicted projections of these variables for the signal and the two unconstrained backgrounds in Figure 3. For this fit we require the secondary vertex confidence level to be greater than 40% where the excess of data over the Monte Carlo prediction is only 10% (see Figure 2b).

The fit attributed the bulk (79±21%) of the ϕ yield to the $D_s^+ \to \phi\mu^+\nu$ signal‡‡. Figure 4 shows the projections of the fit results overlayed on the data.

We next turn to the denominator of our branching ratio measurement, the yield of $D_s^+ \to \phi\pi^+$ events. This sample is obtained with the same selection criteria and uses the

---

**We have recently been made aware of a paper by the Fermilab E653 Collaboration (K. Kodama et al.), to be printed in Physics Letters B, which reports on a first measurement of the R_2 and R_v form factors for $D_s^+ \to \phi\mu^+\nu$. When we redo our analysis using the E653 form factors our branching ratios change by less than 5 %

††We use the decay intensity which is described in [8], our measurement [4] of the form factors R_2 and R_v, and the customary values of 2.5 GeV and 2.1 GeV for the mass of the axial and vector form factors.

‡‡The remaining fraction was nearly equally divided between the backgrounds except $D_s^+ \to \phi\pi^+\pi^-\pi^+$ and $D^+ \to \phi\overline{K}^0\mu^+\nu$ which were found to be negligible.

same vertexing technique as used for our $\phi\mu^+\nu$ sample but with a detachment cut of $\ell/\sigma > 5$ rather than the $\ell/\sigma > 3$ detachment cut used throughout the $\phi\mu^+\nu$ analysis. The secondary vertex confidence level cuts and vertex isolation cuts were identical to those used in the $\phi\mu^+\nu$ analysis. In order to estimate the yield of $D_s^+ \to \phi\pi^+$ events we fit the K^+K^- invariant mass distribution for the sideband subtracted [§§] sample of $D_s^+ \to K^+K^-\pi^+$ decays. A fit to the ϕ peak gives 301 ± 23 $\phi\pi^+$ events and is shown in Figure 5.

Using the observed yield of $D_s^+ \to \phi\mu^+\nu$ candidates, our fit for the level of background contamination, and the fitted yield of $D_s^+ \to \phi\pi^+$ decays we obtain a relative branching ratio of $\Gamma(D_s^+ \to \phi\mu^+\nu)\ /\ \Gamma(D_s^+ \to \phi\pi^+) = 0.58 \pm 0.17$ (stat) $\pm$ 0.07 (sys). Note that if the kinematic fit is performed with the assumption that there is no contribution from the suppressed modes $D_s^+ \to \phi\pi^0\mu^+\nu$, $D^+ \to \phi\mu^+\nu$, and $D^+ \to \phi\overline{K}^0\mu^+\nu$, we find the branching ratio is $0.62 \pm 0.11 \pm 0.07$.

We have included a 21 % correction for the accumulation of low secondary confidence level events (see Figure 2b) which persists beyond a confidence level of 20%. We attribute a 10% systematic error to this subtraction by varying the assumptions used to normalize the curves at large secondary confidence level cut.

Other systematic sources include uncertainty in the scattering or absorption of the pion in the $D_s^+ \to \phi\pi^+$ decay, and uncertainties in the experimental trigger response. A comparison of our branching ratio result to other recent results is presented in Table 1.

It has become customary [5] [6] [9] to use the this branching ratio to infer the $D_s^+ \to \phi\pi^+$ absolute branching ratio. The branching ratio can be computed via the expression:

$$\frac{\Gamma(D_s^+ \to \phi\pi^+)}{\Gamma(D_s^+ \to \text{all})} = \frac{\Gamma(D_s^+ \to \phi\pi^+)}{\Gamma(D_s^+ \to \phi\mu^+\nu)} \frac{\Gamma(D_s^+ \to \phi\mu^+\nu)}{\Gamma(D^+ \to \overline{K}^{*0}\mu^+\nu)} \frac{\Gamma(D^+ \to \overline{K}^{*0}\mu^+\nu)}{\Gamma(D^+ \to \text{all})} \frac{\tau(D_s^+)}{\tau(D^+)}$$

The second factor relating the dominant semileptonic widths of of the D^+ and D_s^+ is expected [1] to range from 0.78 to 1.02. We will use 0.90 ± 0.12. We use a lifetime ratio

---

[§§]For this fit, the D_s^+ signal region is $1.950 < M(K^+K^-\pi^+) < 1.988$ and the sidebands are $1.912 < M(K^+K^-\pi^+) < 1.931$ and $2.007 < M(K^+K^-\pi^+) < 2.026$ (GeV/c^2)

taken from our recent measurement [10] of the D_s^+ lifetime ($0.475 \pm 0.02 \pm 0.007$ ps) and the world average [1] lifetime for the D^+. The $D^+ \to \overline{K}^{*0}\mu^+\nu$ branching ratio is obtained using our recent measurement [4] of the $D^+ \to \overline{K}^{*0}\mu^+\nu$ branching ratio relative to $K^-\pi^+\pi^+$ and the present world average [1] absolute branching ratio for $D^+ \to K^-\pi^+\pi^+$. Our result is $\Gamma(D_s^+ \to \phi\pi^+)/\Gamma(D_s^+ \to \text{all }) = 0.031 \pm 0.009(\text{stat}) \pm 0.005$ (sys) ± 0.004 (theoretical). The present world average [1] on this absolute branching ratio is 0.028 ± 0.005.

In summary, we report a new measurement of the branching ratio $\Gamma(D_s^+ \to \phi\mu^+\nu)/\Gamma(D_s^+ \to \phi\pi^+) = 0.58 \pm 0.17$ (stat) ± 0.07 (sys). In the first published analysis of its kind, a fit to the lifetime and decay kinematics and known background branching ratios was used to estimate the fraction of $\phi\mu^+$ candidates events due to $D_s^+ \to \phi\mu^+\nu$ decays.

This branching ratio is combined with theoretical inputs to obtain a new measurement of the D_s^+ absolute branching ratio of $\Gamma(D_s^+ \to \phi\pi^+)/\Gamma(D_s^+ \to \text{all }) = 0.031 \pm 0.009(\text{stat}) \pm 0.005$ (sys) ± 0.004 (theoretical).

We wish to acknowledge the assistance of the staff of Fermi National Accelerator Laboratory, the INFN of Italy, and the staffs of the physics departments of the collaborating institutions. This research was supported in part by the National Science Foundation, the U.S. Department of Energy, the Italian Istituto Nazionale di Fisica Nucleare and Ministero dell'Università e della Ricerca Scientifica, and the Korean Science and Engineering Foundation.

REFERENCES

[a] Present address: University of Maryland, College Park, MD, 20742,USA

[b] Present address: University of Colorado, Boulder, CO 80309, USA

[c] Present address: Dip. di Fisica Nucleare e Teorica and INFN - Pavia, I-27100 Pavia, Italy

[d] Present address: Fermilab, Batavia, IL 60510, USA.

[e] Present address: University of New York, Stony Brook, NY 11794, USA.

[f] Present address: Yale University, New Haven, CN 06511, USA.

[1] Particle Data Group, K. Hikasa et al., Phys. Rev. D 45 S1 (1992).

[2] M.Wirbel, et al. Z. Phys. C29, 637 (1985)
N. Isgur et al. Phys. Rev. D39 , 799 (1989)

[3] E687 Collab., P. L. Frabetti et al., Nucl. Instrum. Methods. A320 (1992) 519.

[4] E687 Collab., P.L. Frabetti et al., Phys. Lett. B307 (1993) 262

[5] E691 Collab., J. C. Anjos et al., Phys. Rev. Lett. 64 (1990) 2885.

[6] CLEO Collab., J. Alexander et al. Phys Rev Lett. 65 (1990) 1531.

[7] C. W. Bernard et al. Phys Rev. D 45 (1992) 869
V. Lubicz et al. Phys. Lett. B 274 (1992) 415.

[8] E691 Collab., J. C. Anjos et al., Phys. Rev. Lett. 65 (1990) 2630.

[9] ARGUS Collab., H. Albrecht et al., Phys Lett. B 255 (1991) 634.

[10] E687 Collab., P.L. Frabetti et al., submitted to Phys. Rev. Lett. Fermilab-Pub-93/030-E

FIGURES

FIG. 1. The K^-K^+ invariant mass distributions for $D_s^+ \to \phi\mu^+\nu$ candidates with secondary vertex separation cuts a) $\ell/\sigma > 3$, b) $\ell/\sigma > 6$, c) $\ell/\sigma > 9$, and d) $\ell/\sigma > 12$. Fits are shown as solid lines.

FIG. 2. Yields for $D_s^+ \to \phi\mu^+\nu$ as a function of a) the ℓ/σ cut, and b) the secondary vertex confidence level cut. The D_s^+ Monte Carlo prediction is the solid lines. A general $c\bar{c}$ Monte Carlo prediction is the dashed line.

FIG. 3. Predicted distributions for the four kinematic variables used to distinguish the $D_s^+ \to \phi\mu^+\nu$ from the backgrounds $D_s^+ \to \phi\pi^0\mu^+\nu$, and $D^+ \to \phi\overline{K}^0\mu^+\nu$. The four variables are a) the $\phi\mu$ invariant mass, b) the vector meson decay angular variable, $cos\ \theta_v$. c) the weak decay angular variable, $cos\ \theta_\mu$, and d) the reconstructed $\phi\mu\nu$ proper time.

FIG. 4. Comparison of the observed kinematic distributions to the predictions of the background fit described in text. The data are shown as the points with error bars and the fit result is shown as the histogram. The four variables are a) the $\phi\mu$ invariant mass, b) $cos\ \theta_v$. c) $cos\ \theta_\mu$, and d) $\phi\mu\nu$ proper time.

FIG. 5. The D_s^+ sideband subtracted K^+K^- invariant mass distribution used to extract the yield of $D_s^+ \to \phi\pi^+$ events. The curve represents a fit Breit-Wigner ϕ peak over a polynomial background.

TABLES

TABLE I. Measurements of $\Gamma(D_s^+ \to \phi l^+ \nu)/\Gamma(D_s^+ \to \phi\pi^+)$, $l = e$ or μ

	Mode	Signal	$\Gamma(D_s^+ \to \phi l^+ \nu)/\Gamma(D_s^+ \to \phi\pi^+)$
This paper	μ	97 ± 28	$0.58 \pm 0.17 \pm 0.07$
E691 [5]	e	-	< 0.45
CLEO [6]	μ, e avg	54 ± 11	$0.49 \pm 0.10\ ^{+0.10}_{-0.14}$
ARGUS [9]	e	104 ± 26	$0.57 \pm 0.15 \pm 0.15$

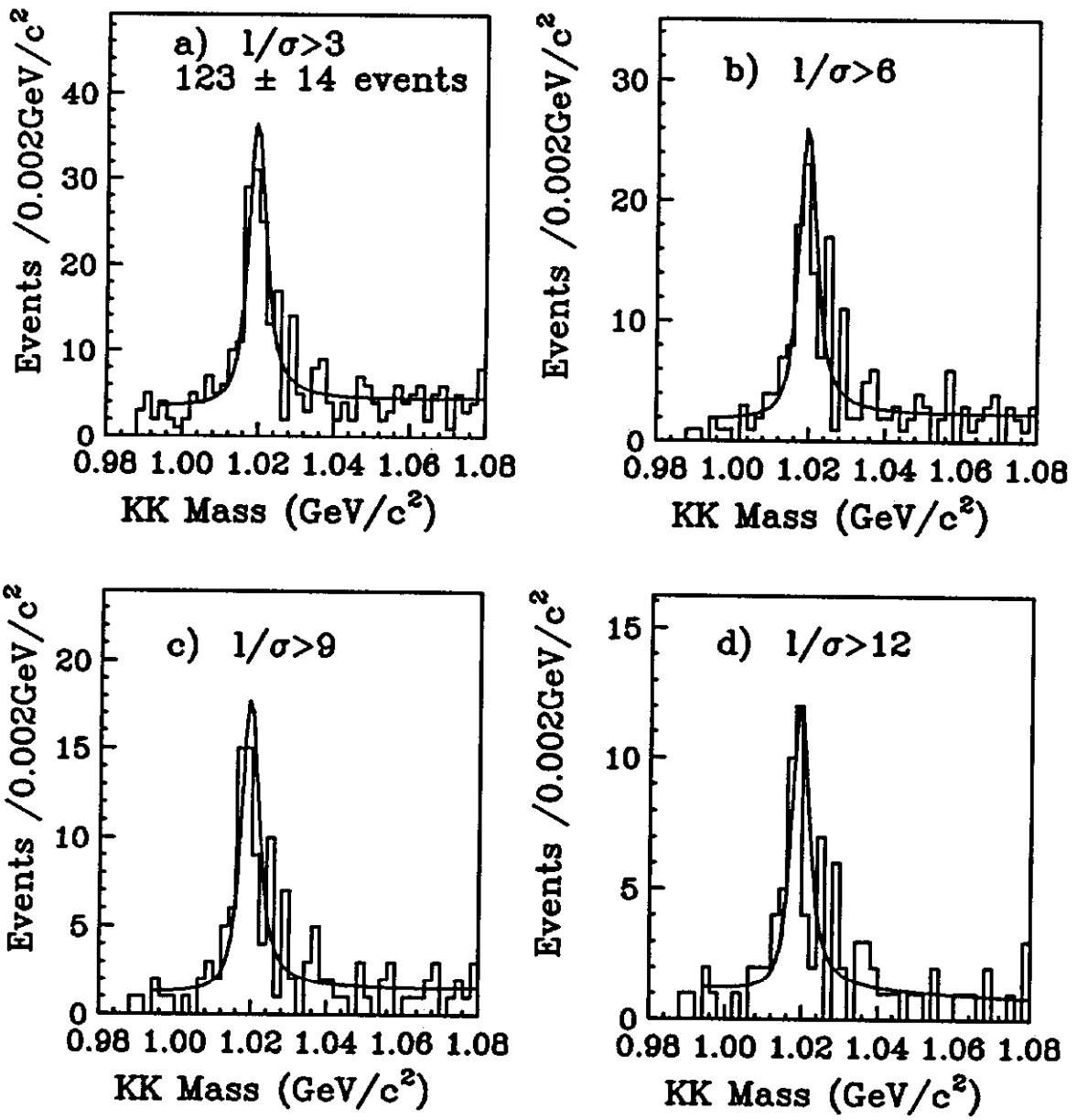

FIG. 1. The K^-K^+ invariant mass distributions for $D_s^+ \to \phi\mu^+\nu$ candidates with secondary vertex separation cuts a) $\ell/\sigma > 3$, b) $\ell/\sigma > 6$, c) $\ell/\sigma > 9$, and d) $\ell/\sigma > 12$. Fits are shown as solid lines.

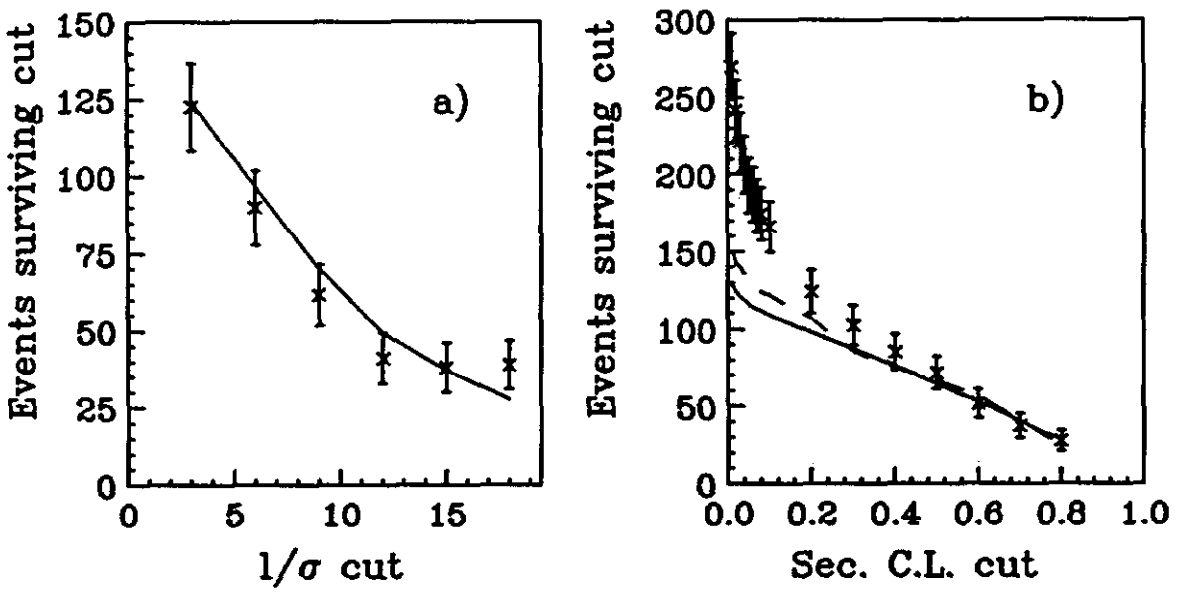

FIG. 2. Yields for $D_s^+ \to \phi\mu^+\nu$ as a function of a) the ℓ/σ cut, and b) the secondary vertex confidence level cut. The D_s^+ Monte Carlo prediction is the solid lines. A general $c\bar{c}$ Monte Carlo prediction is the dashed line.

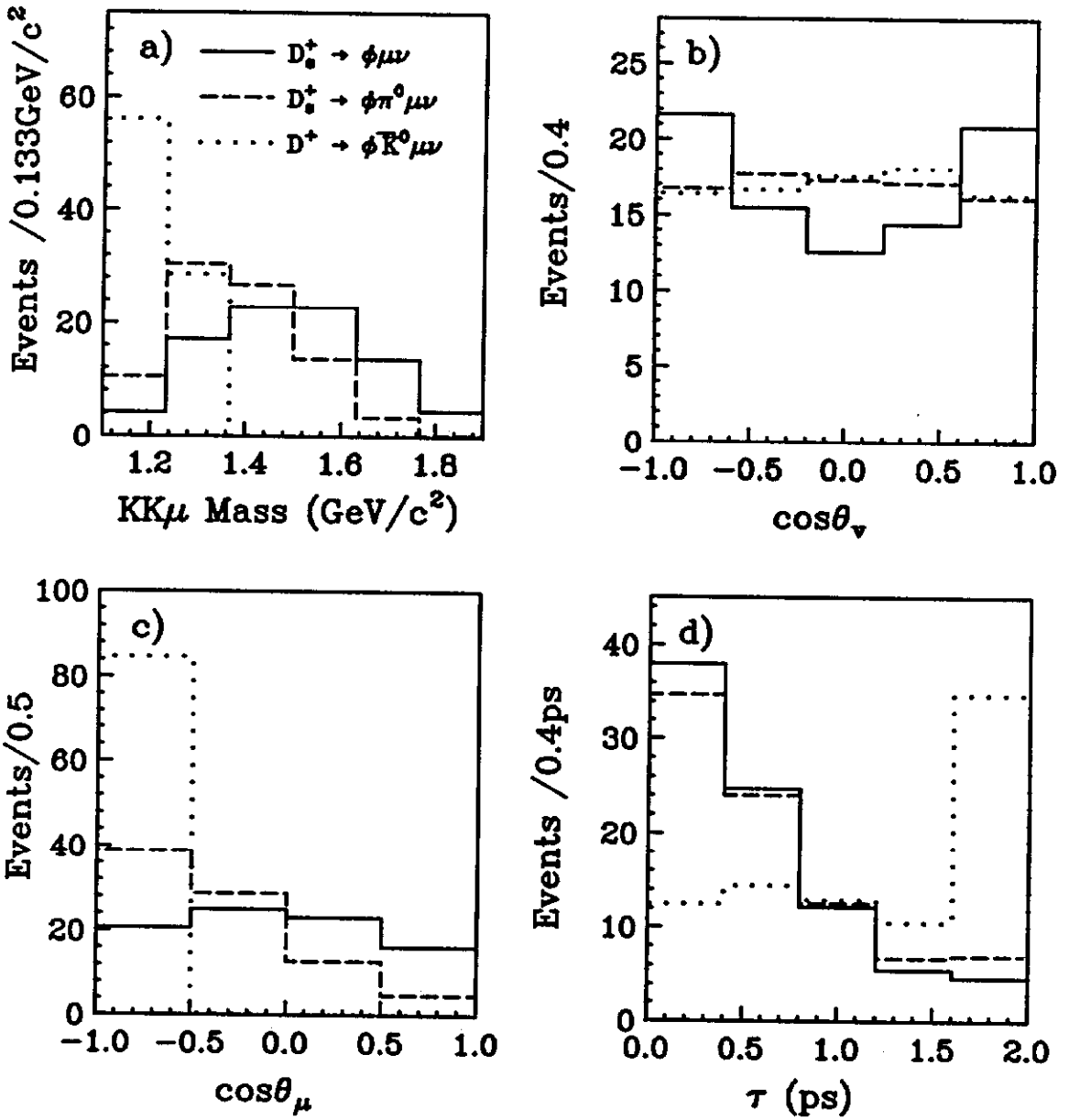

FIG. 3. Predicted distributions for the four kinematic variables used to distinguish the $D_s^+ \to \phi\mu^+\nu$ from the backgrounds $D_s^+ \to \phi\pi^0\mu^+\nu$, and $D^+ \to \phi\overline{K}^0\mu^+\nu$. The four variables are a) the $\phi\mu$ invariant mass, b) the vector meson decay angular variable, $cos\ \theta_v$. c) the weak decay angular variable, $cos\ \theta_\mu$, and d) the reconstructed $\phi\mu\nu$ proper time.

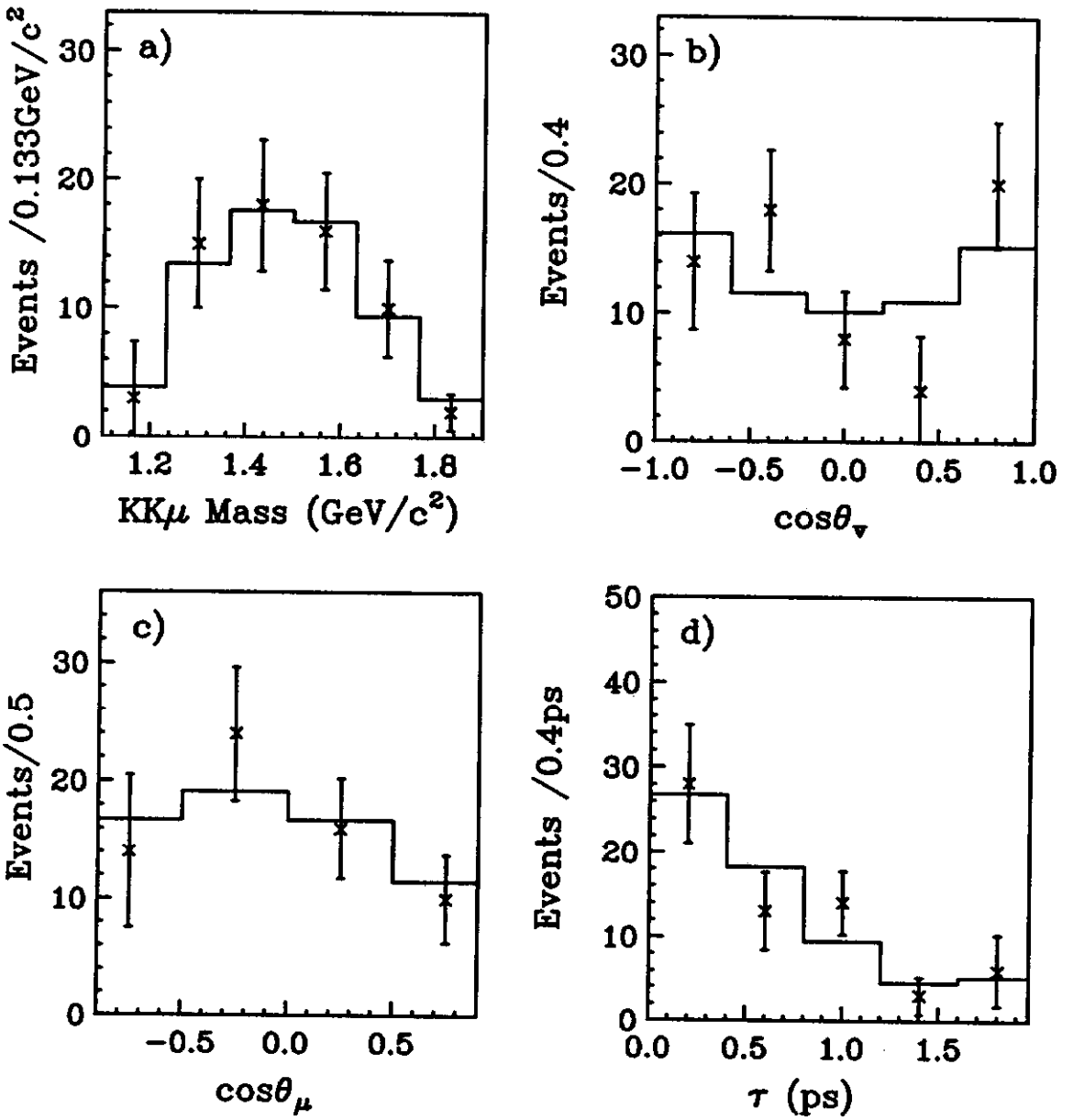

FIG. 4. Comparison of the observed kinematic distributions to the predictions of the background fit described in text. The data are shown as the points with error bars and the fit result is shown as the histogram. The four variables are a) the $\phi\mu$ invariant mass, b) $cos\ \theta_\nu$. c) $cos\ \theta_\mu$, and d) $\phi\mu\nu$ proper time.

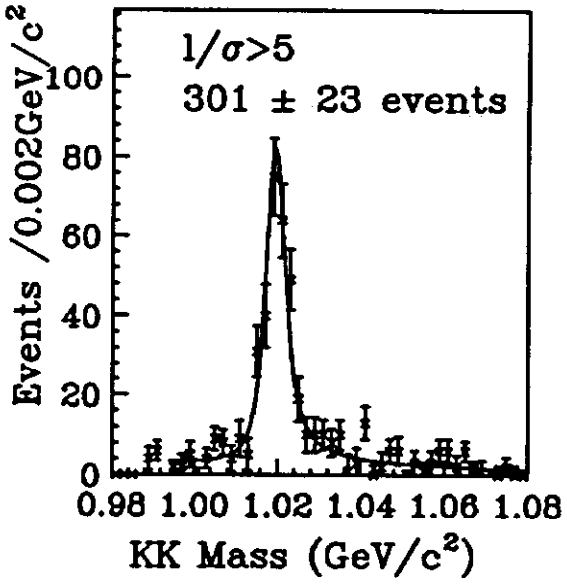

FIG. 5. The D_s^+ sideband subtracted K^+K^- invariant mass distribution used to extract the yield of $D_s^+ \to \phi\pi^+$ events. The curve represents a fit Breit-Wigner ϕ peak over a polynomial background.